

The Rate-Limiting Step of O₂ Activation in the α -Ketoglutarate Oxygenase Factor Inhibiting Hypoxia Inducible Factor

John A. Hangasky,[†] Hasand Gandhi,[‡] Meaghan A. Valliere,[†] Nathaniel E. Ostrom,[‡] and Michael J. Knapp^{*,†}

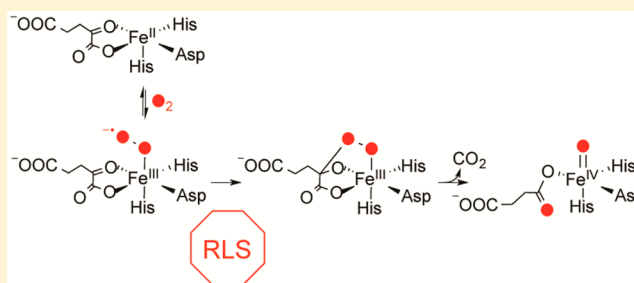
[†]Department of Chemistry, University of Massachusetts, Amherst, Massachusetts 01003, United States

[‡]Department of Zoology, Michigan State University, East Lansing, Michigan 48824, United States

S Supporting Information

ABSTRACT: Factor inhibiting HIF (FIH) is a cellular O₂-sensing enzyme, which hydroxylates the hypoxia inducible factor-1 α . Previously reported inverse solvent kinetic isotope effects indicated that FIH limits its overall turnover through an O₂ activation step (Hangasky, J. A., Saban, E., and Knapp, M. J. (2013) *Biochemistry* 52, 1594–1602). Here we characterize the rate-limiting step for O₂ activation by FIH using a suite of mechanistic probes on the second order rate constant $k_{\text{cat}}/K_{\text{M}(\text{O}_2)}$. Steady-state kinetics showed that the rate constant for O₂ activation was slow ($k_{\text{cat}}/K_{\text{M}(\text{O}_2)}^{\text{app}} = 3500 \text{ M}^{-1} \text{ s}^{-1}$) compared

with other non-heme iron oxygenases, and solvent viscosity assays further excluded diffusional encounter with O₂ from being rate limiting on $k_{\text{cat}}/K_{\text{M}(\text{O}_2)}$. Competitive oxygen-18 kinetic isotope effect measurements ($^{18}k_{\text{cat}}/K_{\text{M}(\text{O}_2)} = 1.0114(5)$) indicated that the transition state for O₂ activation resembled a cyclic peroxohemiketal, which precedes the formation of the ferryl intermediate observed in related enzymes. We interpret this data to indicate that FIH limits its overall activity at the point of the nucleophilic attack of Fe-bound O₂⁻ on the C-2 carbon of α KG. Overall, these results show that FIH follows the consensus mechanism for α KG oxygenases, suggesting that FIH may be an ideal enzyme to directly access steps involved in O₂ activation among the broad family of α KG oxygenases.



Mammalian cells respond to decreased cellular pO₂ levels through the enzyme-catalyzed reaction of O₂ with the hypoxia inducible factor-1 α (HIF-1 α or HIF).¹ HIF mediates the transcription of hundreds of genes in response to hypoxia² with the functions of the gene products ranging from glucose and iron metabolism to cell proliferation and angiogenesis.^{3,4} Factor inhibiting HIF (FIH) is a non-heme Fe(II)/ α KG oxygenase that turns-off the transcriptional activity of HIF^{5,6} by hydroxylating the β -carbon of Asn⁸⁰³ within the C-terminal activation domain (CTAD) of HIF (Scheme 1).^{7–9} Because O₂ activation chemistry is central to hypoxia sensing by HIF, identifying the chemical steps involved in O₂ activation may point the way to methods for perturbing HIF-controlled gene expression.

FIH is proposed to follow the consensus mechanism for Fe(II)/ α KG oxygenases (Scheme 1) for which the steps are supported to varying degrees by spectroscopic, computational, and kinetic studies.^{10–15} VTVH MCD methodologies have been used to spectroscopically identify the release of the aquo ligand upon substrate binding to FIH¹⁶ and other Fe(II)/ α KG oxygenases including TauD and CAS.^{17,18} O₂ is thought to bind as a ferric superoxide at the open coordination site and then attacks the C-2 carbonyl of α KG to ultimately form succinate and a ferryl intermediate. The molecular details following O₂ activation, including isolation of the ferryl intermediate and

observation of HAT have been characterized in the Fe(II)/ α KG oxygenases TauD^{15,19–24} and P4H²⁵ and the related Fe(II)/ α KG halogenases CytC3²⁶ and SyrB2.²⁷

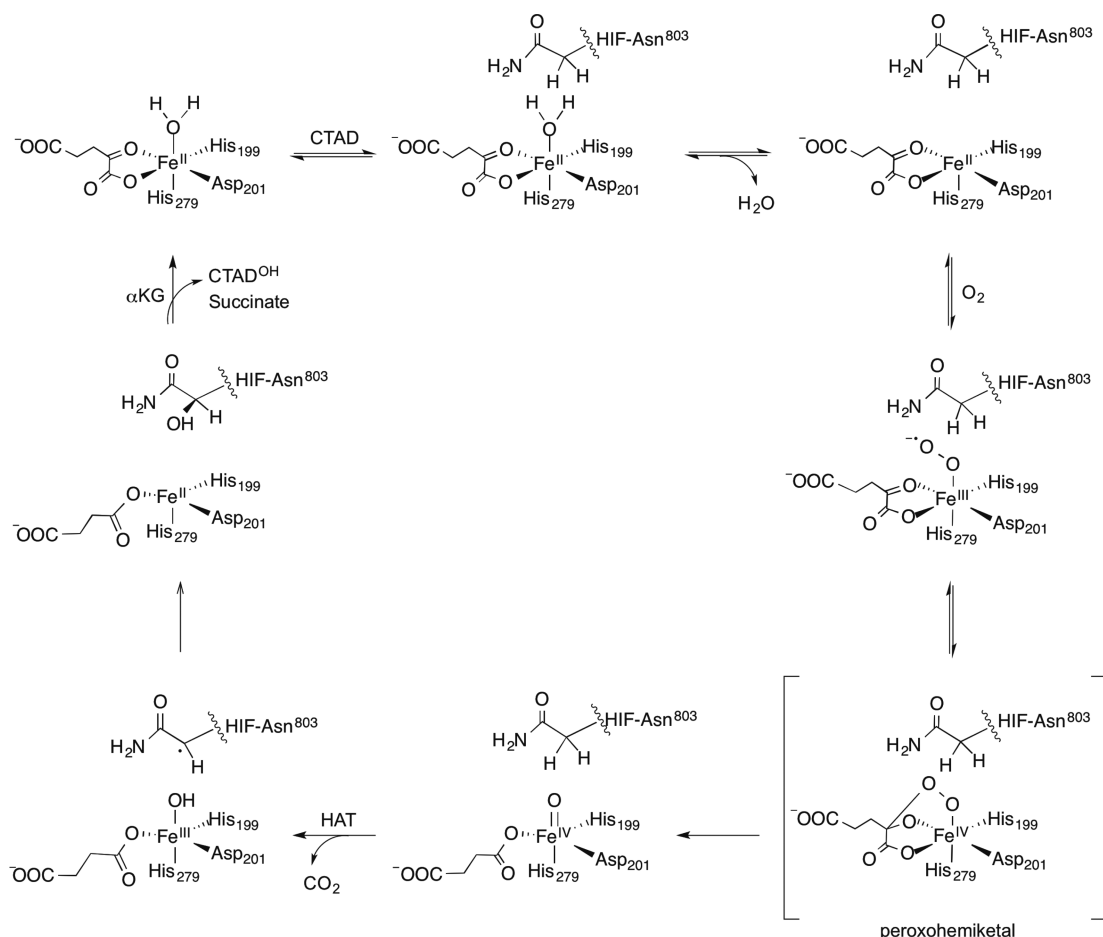
In contrast to the steps following ferryl formation, those steps of O₂ activation are poorly understood. Computational studies suggest that nucleophilic attack on the C-2 carbonyl of α KG is the rate-limiting step on $k_{\text{cat}}/K_{\text{M}(\text{O}_2)}$, with a cyclic peroxohemiketal proposed as the transition state.^{28–30} Although this reaction sequence is supported by pre-steady-state kinetics and an oxygen-18 kinetic isotope effect (¹⁸O KIE) study of TauD,³¹ insight into O₂ activation is limited because HAT or product release is rate-limiting in TauD and other well-characterized α KG oxygenases.^{20,32,33} Consequently, O₂ activation is too rapid to allow for the identification of any intermediates prior to the ferryl.

Recent studies showed that the rate-limiting step for FIH differed from that of other characterized α KG oxygenases.^{16,34} Upon FIH binding to CTAD, there is partial retention of the aquo ligand¹⁶ suggesting that aquo release may be less facile in FIH than in other enzymes. The inverse SKIE on k_{cat} ³⁴ for FIH

Received: October 2, 2014

Revised: November 20, 2014

Published: November 25, 2014

Scheme 1. Consensus Chemical Mechanism of α KG Oxygenases, Adapted for FIH

indicates that the aquo release reaches equilibrium prior to an irreversible step that is the overall rate-limiting step in FIH; in other words, the overall rate limiting step either precedes or coincides with the formation of the ferryl. This suggests that FIH either deviates from the consensus chemical mechanism or could provide a unique system to access other steps of mechanistic interest. In this work, we probe $k_{\text{cat}}/K_{\text{M}(\text{O}_2)}$, which focuses on the limited subset of steps that are involved in binding and reacting with O_2 , to understand O_2 activation by FIH. Steady-state kinetics under conditions of varied solvent viscosity indicated that diffusional encounter of O_2 with FIH was not rate limiting on $k_{\text{cat}}/K_{\text{M}(\text{O}_2)}$. Furthermore, we determined the ^{18}O KIE on $k_{\text{cat}}/K_{\text{M}(\text{O}_2)}$ ($^{18}k_{\text{cat}}/K_{\text{M}(\text{O}_2)} = 1.0114(5)$), identifying the rate-limiting step as formation of the peroxohemiketal. This showed that the chemical steps of O_2 activation on FIH followed the consensus mechanism, indicating that FIH only differs from other α KG oxygenases in that this O_2 activation step is the overall rate-limiting step during turnover.³⁴

MATERIALS AND METHODS

Materials. All reagents were purchased from commercial sources and used as received unless noted. The sequences of the synthetic 19- and 39-mer CTAD peptides corresponded to the C-terminal activation domain (CTAD) of HIF-1 α ^{788–806} and HIF-1 α ^{788–826}, respectively, with a Cys⁸⁰⁰ → Ala point mutation. Peptides were purchased from EZBiolab (Carmel,

Indiana, USA) with free N- and C-termini. The CTAD^{788–806} peptide (purity >95%) was used without further purification; however CTAD^{788–826} was purchased as a desalted peptide and purified to >95% purity using RP-HPLC as previously described.³⁴

Protein Expression and Purification. FIH was overexpressed in *Escherichia coli* and purified as previously reported.^{34,35} Thrombin cleavage of the His₆ tag led to three additional residues preceding the native sequence of FIH on the N-terminus (NH₂-Gly-Ser-His-). The purity of the protein (>95%) was assessed through SDS-PAGE.

Steady-State Kinetic Assays with Varying O_2 . All assays were performed in an AtmosBag (Sigma-Aldrich) with the O_2 concentration of the reaction buffers equilibrated to the O_2 partial pressure within the bag. The atmosphere of the bag was equilibrated for 30 min with a controlled mixture of N_2 and O_2 . HEPES, pH 7.00 (50 mM) was gently stirred for 5 min in a 37.0 °C water bath to equilibrate the reaction buffer with the atmosphere, and then the O_2 concentration was measured using a Clarke electrode.

Steady-state assays in which O_2 was the varied substrate (0.020–1 mM) utilized a fixed CTAD^{788–826} concentration of either 80 μM ($\sim K_{\text{M}(\text{CTAD})}$) or 150 μM ($\sim 2K_{\text{M}(\text{CTAD})}$) and saturating concentrations of FeSO_4 (25 μM), α KG (100 μM), and ascorbate (2 mM), prepared in 50 mM HEPES, pH 7.00. Upon addition of all reagents except FIH, the reaction mixture (45 μL) was incubated at 37.0 °C for an additional 2 min. The enzyme stock was equilibrated to the atmosphere by gently

pipetting the solution down the side of the microcentrifuge tube, before injecting an aliquot (5 μL) to initiate the assays. Reaction aliquots were removed throughout a 3 min time course, quenched in 75% acetonitrile/0.2% TFA (20 μL) saturated with 3,5-dimethoxy-4-hydroxycinnamic acid and analyzed for the initial rate of formation of CTAD^{OH} using a Bruker microFlex MALDI-TOF-MS. Initial rates were determined as previously described³⁴ and fit to the Michaelis–Menten equation resulting in the apparent kinetic parameters k_{cat} , $k_{\text{cat}}/K_{\text{M}(\text{O}_2)}$, and $K_{\text{M}(\text{O}_2)}$.

Solvent Viscosity Effect. Assays to test for rate-limiting diffusional encounter of O₂ utilized a fixed CTAD^{788–826} concentration of 80 μM ($\sim K_{\text{M}(\text{CTAD})}$) and saturating concentrations of FeSO₄ (25 μM), αKG (100 μM), and ascorbate (2 mM), with the exception of the addition of sucrose (25% w/w) to the 50 mM HEPES, pH 7.00, to give a relative viscosity of $\eta/\eta_0 = 2.4$.³⁶ Reactions were performed as described above to determine initial rates with O₂ as the varied substrate, which were then fit to the Michaelis–Menten equation.

Steady-State Kinetic Assays with CTAD^{788–806}. Assays in which CTAD^{788–806} was varied (0.10–4.6 mM) were performed at 37.0 °C in 50 mM HEPES, pH 7.00, and contained ascorbate (2 mM), αKG (1 mM), FeSO₄ (50 μM), and an ambient O₂ concentration (217 μM). Assays in which αKG was varied (0.005–1 mM) were also performed at 37.0 °C in 50 mM HEPES, pH 7.00, and contained ascorbic acid (2 mM), FeSO₄ (50 μM), and CTAD^{788–806} (750 μM), with an ambient O₂ concentration (217 μM). Reagents were mixed and incubated at 37.0 °C for 2 min before initiating turnover with enzyme (5–20 μM). At predetermined time points, aliquots were quenched in 75% acetonitrile/0.2% TFA (20 μL) saturated with α -cyano-4-hydroxycinnamic acid. Initial rates were determined as described above and fit to the Michaelis–Menten equation resulting in the apparent kinetic parameters k_{cat} , $k_{\text{cat}}/K_{\text{M}}$, and K_{M} .

¹⁸O KIE Sample Preparation and Analysis. Assays used to determine the ¹⁸O KIE contained αKG (1.0 mM), CTAD^{788–806} (250 μM), FeSO₄ (50 μM), and O₂ (280 μM) in 50 mM HEPES, pH 7.00. Buffer was equilibrated to ambient O₂ concentration (280 μM) by gently stirring for 2 days at 21 °C. All reagents were prepared freshly using the equilibrated buffer and gently mixed to make a common reaction mixture. This reaction mixture was injected into a 10 mL crimp vial sealed with a butyl rubber stopper (Geo-Microbial Technologies, Inc.; Ochelata, OK), ensuring all air was removed. After a 3 min incubation of the vial at 37.0 °C, each reaction was initiated with an injection (20 μL) of a high concentration FIH stock that had been equilibrated to room temperature (21 °C). Reactions were quenched using 6 M HCl, 3.5 M ZnCl₂ (40 μL) after an extended reaction time such that the fractional conversion based on O₂ was as high as 35%. An aliquot (5 μL) was removed to determine the reaction progress by measuring CTAD^{OH} formation using a Bruker MALDI-TOF-MS. The quantity of CTAD^{OH} produced was used to determine the fractional conversion of O₂ for each quenched reaction. The sealed crimp vials containing the quenched reactions were stored inverted and submerged in water until analysis by isotope-ratio mass spectrometry (IRMS).

The ¹⁸O KIE samples were carefully transferred into pre-evacuated 25 mL glass vessels fitted with a glass high vacuum stopcock (Chemglass). The filling procedure is described in

detail by Emerson et al.³⁷ but briefly consisted of flushing the neck of the bottle with a gentle stream of CO₂ to displace air followed by introduction of sample water from a small diameter tubing (~ 3 mm) to the bottleneck. Upon opening the stopcock slowly, sample water is drawn into the evacuated bottle until the bottle is approximately half full. The headspace gases and water are then equilibrated by gently shaking in a 25 °C water bath overnight. Before IRMS analysis, the sample water was removed using aspiration, leaving ~ 0.5 mL of sample in the bottle. Headspace gases in the bottle were then analyzed for the $\delta^{18}\text{O}$ of O₂ using a gas chromatograph interfaced to an Elementar Isoprime IRMS.³⁸ All $\delta^{18}\text{O}$ isotopic values were reported using standard delta notation relative to the Vienna standard mean ocean water (VSMOW).³⁹ Equation 1 was used to convert the $\delta^{18}\text{O}$ to an R value (¹⁸O/¹⁶O isotopic ratio), where R_{std} is the standard isotopic value for O₂ in air (0.0020531)⁴⁰ and R_f is the ¹⁸O/¹⁶O isotopic ratio at O₂ fractional conversion f .

$$R_f = \left(\frac{\delta^{18}\text{O}}{1000} + 1 \right) R_{\text{std}} \quad (1)$$

To determine the ¹⁸O/¹⁶O isotopic ratio at $t = 0$ (R_0), a sample was prepared from the common reaction stock containing αKG (1.0 mM), CTAD^{788–806} (250 μM), FeSO₄ (50 μM), and O₂ (280 μM) in 50 mM HEPES, pH 7.00, and injected into a sealed crimp vial. After incubation for 3 min at 37.0 °C, an aliquot of 50 mM HEPES, pH 7.00 (20 μL), was injected into the vial immediately followed by an injection (40 μL) of 6 M HCl, 3.5 M ZnCl₂ to quench the reaction.

The ¹⁸O KIE was determined by fitting R_f/R_0 vs f to eq 2, where f is the fractional conversion of O₂ in the reaction aliquot, R_f is the ¹⁸O/¹⁶O isotope ratio of the aliquot, and R_0 is the ¹⁸O/¹⁶O isotope ratio of the blank.

$$\frac{R_f}{R_0} = (1 - f)^{(1/^{18}\text{O-KIE})-1} \quad (2)$$

RESULTS AND DISCUSSION

The O₂ activation mechanisms of Fe(II)/ αKG oxygenases are of enormous interest due to the biomedical significance of these enzymes.^{12,41,42} FIH hydroxylates the HIF transcription factor for hypoxia sensing, and other members are involved in processes such as DNA and RNA repair and histone demethylation,^{12,43,44} placing some of these enzymes into biological roles that are more concerned with regulation than with bulk turnover of metabolites. A crucial mechanistic feature of these enzymes is O₂ activation to form an active oxidant, identified in several enzymes as a ferryl species.^{19,25,26} Despite the importance of the chemical steps leading up to formation of the ferryl, these steps remain largely uncharacterized. Because the overall rate-limiting step for FIH either precedes or coincides with ferryl formation,³⁴ FIH could be an excellent enzyme to interrogate steps involved in O₂ activation that are common to other αKG oxygenases, provided that FIH follows the consensus mechanism.

Steady-State Kinetics with Varying O₂. To characterize the steps limiting the rate of O₂ activation by FIH, steady-state kinetic assays with O₂ as the varied substrate were performed using a fixed CTAD^{788–826} concentration. Because our assays used subsaturating CTAD concentration due to reagent expenses, these steady-state assays used two different

CTAD^{788–826} concentrations to measure the second order rate constant, $k_{\text{cat}}/K_{\text{M}(\text{O}_2)}$.

The initial rate data using 80 μM CTAD^{788–826} was fit to the Michaelis–Menten equation with kinetic parameters of $k_{\text{cat}}^{\text{app}} = 33 \pm 3 \text{ min}^{-1}$ and $k_{\text{cat}}/K_{\text{M}(\text{O}_2)}^{\text{app}} = 0.17 \pm 0.03 \mu\text{M}^{-1} \text{ min}^{-1}$ (Figure 1, Table 1). The steady-state assays with varying O_2

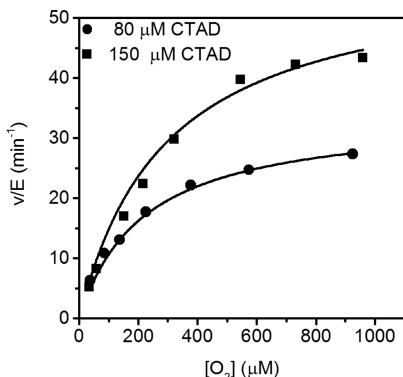


Figure 1. Steady-state kinetics with varying O_2 . Reactions contained FIH (0.25–0.5 μM), ascorbate (2 mM), αKG (100 μM), FeSO_4 (25 μM), and CTAD^{788–826} (80 μM , ●, or 150 μM , ■) in 50 mM HEPES, pH 7.00, 37.0 °C.

Table 1. Apparent Kinetic Parameters for FIH with Varied O_2 Concentration^a

[CTAD ^{788–826}] (μM)	$k_{\text{cat}}^{\text{app}}$ (min^{-1})	$k_{\text{cat}}/K_{\text{M}(\text{O}_2)}^{\text{app}}$ ($\mu\text{M}^{-1} \text{ min}^{-1}$)	$K_{\text{M}(\text{O}_2)}^{\text{app}}$ (μM)
80	33 ± 3.0	0.17 ± 0.03	200 ± 40
150	54 ± 4.0	0.21 ± 0.04	270 ± 50

^aReactions contained ascorbate (2 mM), αKG (100 μM), FeSO_4 (25 μM), and CTAD^{788–826} in 50 mM HEPES, pH 7.00, 37.0 °C.

using an increased CTAD concentration (150 μM) resulted in $k_{\text{cat}}/K_{\text{M}(\text{O}_2)}^{\text{app}} = 0.21 \pm 0.04$, which is statistically equivalent to the $k_{\text{cat}}/K_{\text{M}(\text{O}_2)}^{\text{app}}$ at 80 μM CTAD^{788–826}. These results indicated that $k_{\text{cat}}/K_{\text{M}(\text{O}_2)}$ was independent of CTAD concentration as expected for the sequential consensus mechanism (Scheme 1). The high value for the Michaelis constant ($K_{\text{M}(\text{O}_2)}^{\text{app}} > 200 \mu\text{M}$) was in agreement with previous reported values (90–237 μM) obtained using oxygen consumption assays and ¹⁴CO₂ capture assays^{45,46} and is thought to be essential for a proportionate sensory response by FIH to increasing pO₂.

When converted into standard units, $k_{\text{cat}}/K_{\text{M}(\text{O}_2)}^{\text{app}} = 3.5 \times 10^3 \text{ M}^{-1} \text{ s}^{-1}$, it was clear that the rate constant for O_2 activation in FIH was significantly slower than those for non-heme iron oxygenases that are not involved in O_2 concentration sensing, such as TauD ($1.5 \times 10^5 \text{ M}^{-1} \text{ s}^{-1}$),^{33,47} tyrosine hydroxylase ($6.0 \times 10^4 \text{ M}^{-1} \text{ s}^{-1}$),⁴⁸ and lipoxygenase ($\sim 5.0 \times 10^5 \text{ M}^{-1} \text{ s}^{-1}$).^{49,50} In contrast, the slow rate constant for O_2 activation and the high Michaelis constant for O_2 found for FIH are found in those non-heme iron oxygenases implicated in O_2 sensing, such as PHD2⁵¹ and Jumonji C domain-containing histone demethylases.⁵² The small magnitude of $k_{\text{cat}}/K_{\text{M}(\text{O}_2)}$ for FIH is intriguing, raising the potential for FIH and these putative O_2 sensors to use an unusual strategy for O_2 activation. Although it is likely that a slow chemical step limits $k_{\text{cat}}/K_{\text{M}(\text{O}_2)}$ and O_2

activation, it was necessary to test diffusional encounter as a possibility for the rate-limiting step.

Solvent Viscosity Effect. To test for diffusional encounter with O_2 as a partially rate-limiting step on $k_{\text{cat}}/K_{\text{M}(\text{O}_2)}$, we performed steady-state assays under varied solvent viscosity. Although $k_{\text{cat}}/K_{\text{M}(\text{O}_2)}$ is orders of magnitude slower than expected for a diffusional process (ca. $1 \times 10^9 \text{ M}^{-1} \text{ s}^{-1}$), we could not dismiss the possibility that there was an unfavorable pre-equilibrium leading to a very small fraction of FIH being competent for reaction upon collision. For diffusion controlled processes, $k_{\text{cat}}/K_{\text{M}(\text{O}_2)}$ would decrease in the presence of added viscosogen due to a lower diffusion rate as observed for other enzymes such as superoxide dismutase^{53,54} and carbonic anhydrase.^{55,56}

Our assays were performed as described above in the presence and absence of the viscosogen sucrose, giving a final relative viscosity (η/η_0) of 1.0 and 2.4, respectively (Figure 2).

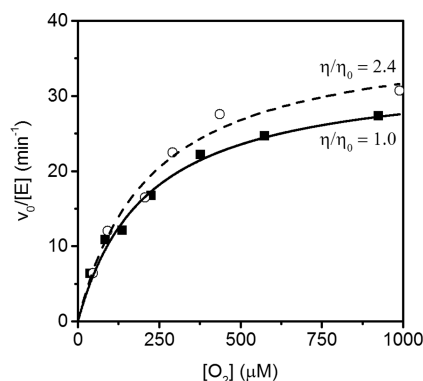


Figure 2. Steady-state kinetics with varying O_2 : 0% sucrose (solid line, $\eta/\eta_0 = 1$) and 25% sucrose (dashed line, $\eta/\eta_0 = 2.4$). Assays contained ascorbate (2 mM), αKG (100 μM), FeSO_4 (25 μM), CTAD^{788–826} (80 μM), and sucrose (0% or 25%) in 50 mM HEPES, pH 7.00, 37.0 °C.

At increased solvent viscosity, the resulting kinetic parameter $k_{\text{cat}}/K_{\text{M}(\text{O}_2)}^{\text{app}} = 0.18 \pm 0.04 \mu\text{M}^{-1} \text{ min}^{-1}$ was indistinguishable from the kinetic parameter collected in the absence of viscosogen (Table 2). The resulting insignificant solvent viscosity effect on $k_{\text{cat}}/K_{\text{M}(\text{O}_2)}$ indicated that diffusional encounter with O_2 did not limit the rate constant for O_2 activation in FIH.

Table 2. Solvent Viscosity Effect on $k_{\text{cat}}/K_{\text{M}(\text{O}_2)}$ ^a

η/η_0	$k_{\text{cat}}^{\text{app}}$ (min^{-1})	$k_{\text{cat}}/K_{\text{M}(\text{O}_2)}^{\text{app}}$ ($\mu\text{M}^{-1} \text{ min}^{-1}$)	$K_{\text{M}(\text{O}_2)}^{\text{app}}$ (μM)
1.0	33 ± 3.0	0.17 ± 0.03	200 ± 40
2.4	39 ± 3.0	0.18 ± 0.04	220 ± 43

^aAssays contained ascorbate (2 mM), αKG (100 μM), FeSO_4 (25 μM), CTAD^{788–826} (80 μM), and sucrose (0% or 25% w/w) in 50 mM HEPES, pH 7.00, 37.0 °C.

Diffusion limited rate constants may be found with enzymes that have achieved catalytic perfection, reflecting a physiological role that requires bulk turnover of a large quantity of substrate. For example, diffusion limited rate constants fit well for SOD's cellular function to scavenge superoxide to minimize oxidative damage.⁵⁷ As an O_2 sensor, one would imagine that FIH turnover could be limited by collisional encounter. However, the absence of a viscosity effect on $k_{\text{cat}}/K_{\text{M}(\text{O}_2)}$ and k_{cat} showed

that FIH was not diffusively limited under varied O_2 concentration. This implicates a chemical step as rate-limiting under conditions of low O_2 concentration, consistent with prior results indicating that k_{cat} was limited by a step that followed aquo release but preceded the HAT.³⁴

Competitive ^{18}O Kinetic Isotope Effect. Because $k_{cat}/K_{M(O_2)}$ encompasses all steps between diffusional collision of FIH with O_2 through the subsequent irreversible step, the ^{18}O heavy atom isotope effect on this rate constant is an ideal reporter of the rate-limiting step. We employed competitive $^{18}O/^{16}O$ KIE measurements using O_2 at natural isotopic abundance to identify the rate limiting step on $k_{cat}/K_{M(O_2)}$ in FIH. The $^{18}O/^{16}O$ isotopic abundance of residual O_2 was measured by IRMS from quenched reactions of FIH, which were fit to eq 2 resulting in a $^{18}k_{cat}/K_{M(O_2)} = 1.0114(5)$ (Figure 3). Because the typical range of values for $^{18}k_{cat}/K_{M(O_2)}$ is 1.00–

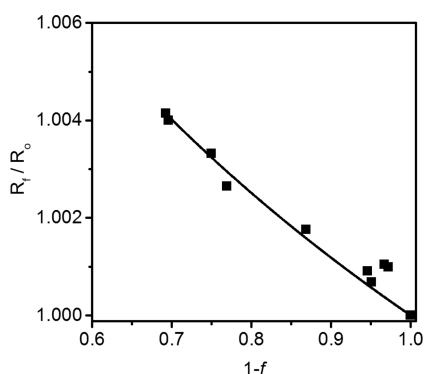
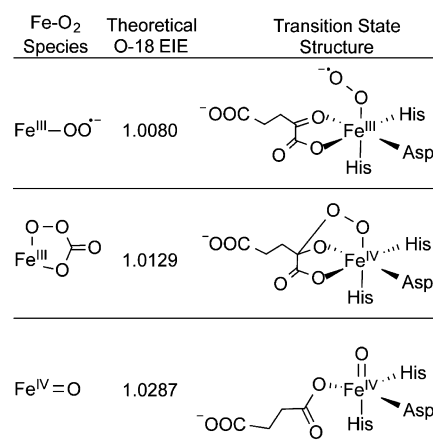


Figure 3. ^{18}O fractionation (R_f/R_o) versus the fractional conversion of O_2 in quenched reactions of FIH. Each reaction contained α KG (1.0 mM), CTAD^{788–806} (250 μ M), $FeSO_4$ (50 μ M), and O_2 (280 μ M) in 50 mM HEPES, pH 7.00, 37.0 °C. Data are fit to eq 2; $^{18}k_{cat}/K_{M(O_2)} = 1.0114(5)$.

1.03, this places O_2 activation by FIH in a clear context when considered next to the mechanisms followed by other non-heme Fe enzymes.³¹

$^{18}k_{cat}/K_{M(O_2)}$ reflects the changes in O–O bonding between molecular O_2 and the transition state of the kinetically irreversible step on $k_{cat}/K_{M(O_2)}$.^{58,59} Because the ^{18}O equilibrium isotope effect (^{18}O EIE) provides an upper limit for the ^{18}O KIE,⁶⁰ previously calculated ^{18}O EIEs for the equilibrium $Fe^{2+} + O_2 \rightleftharpoons X$ provide an excellent yardstick for the transition state structure based upon the value of $^{18}k_{cat}/K_{M(O_2)}$ (Chart 1).³¹ For example, the calculated ^{18}O EIE for $X = Fe^{3+}(O_2^-)$ is small (^{18}O EIE = 1.0080),³¹ meaning that rate-limiting formation of this intermediate would lead to a correspondingly small value for $^{18}k_{cat}/K_{M(O_2)}$. A larger ^{18}O EIE is calculated for $X =$ ferric peroxy-carbonate (^{18}O EIE = 1.0129),³¹ a structure resembling the putative peroxohemiketal, which is in good agreement with the observed $^{18}k_{cat}/K_{M(O_2)}$ for FIH, suggesting that the rate-limiting step for FIH proceeds through a transition state that resembles this structure. In contrast, the observed $^{18}k_{cat}/K_{M(O_2)}$ is inconsistent with the ^{18}O EIE calculated for $X =$ ferryl (^{18}O EIE = 1.0287),³¹ indicating that the ferryl intermediate is formed after the rate-limiting step on $k_{cat}/K_{M(O_2)}$ in FIH.

Chart 1. Proposed Transition State Structures from ^{18}O EIE^a



^a ^{18}O EIE values were calculated in ref 31.

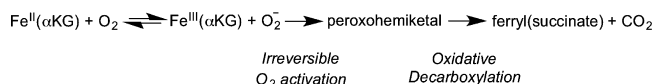
$^{18}k_{cat}/K_{M(O_2)}$ has been utilized to study the O_2 activation pathways of other non-heme iron enzymes including soluble methane monooxygenase,⁶¹ ACCO,⁶² TauD,³¹ HppE,³¹ and tyrosine hydroxylase.⁶³ In each case, the magnitude of $^{18}k_{cat}/K_{M(O_2)}$ provided important insight into the chemical strategy followed for O_2 activation. For those enzymes in which O_2 binds at Fe^{2+} , the initial step is the reversible formation of a $Fe^{3+}(O_2^-)$ adduct, which subsequently requires electrons from cofactor or (co)substrate to activate the O–O bond for chemistry. In the case of TauD, this activation takes the form of a nucleophilic attack of the $Fe^{3+}(O_2^-)$ on the C-2 keto position of α KG.³¹

The $^{18}k_{cat}/K_{M(O_2)}$ for FIH (1.0114(5)) is very similar to that observed for TauD ($^{18}k_{cat}/K_{M(O_2)} = 1.0102$),³¹ indicating a common transition state structure for α KG decarboxylation in these two enzymes. The larger value for the $^{18}k_{cat}/K_{M(O_2)}$ for FIH than for TauD is likely due to the slower turnover rate of FIH. The observed $^{18}k_{cat}/K_{M(O_2)}$ will approach the ^{18}O EIE when the forward commitment, which is the ratio of the forward and reverse rate constants for disappearance of the species immediately preceding the rate-limiting step, is small as might be expected for the slower chemistry in FIH.

The chemical strategy for O_2 activation in α KG oxygenases was predicted by DFT calculations to proceed through the nucleophilic attack on the α KG cofactor^{28,29} and is supported by the ^{18}O KIE results. The self-consistent field (SCF) calculations predicted that decomposition of the initially formed cyclic peroxohemiketal intermediate was barrierless²⁹ leading to decarboxylation with the formation of a Fe^{2+} (peroxysuccinate) intermediate prior to formation of the ferryl(succinate). Because the decarboxylation is irreversible, $k_{cat}/K_{M(O_2)}$ only reports on steps between the collision with O_2 and this decarboxylation step (Scheme 2).

Studies to date that address O_2 activation chemistry in α KG oxygenases have relied on steady-state mechanistic probes and

Scheme 2. O_2 Activation in α KG Oxygenases



point mutagenesis^{22,45,64–67} and suggest that hydrogen bonding contacts to the α KG play an important role in facilitating decarboxylation. Further insight into oxidative decarboxylation has been hampered by the identity of the rate limiting steps in TauD and other α KG oxygenases. In the cases of TauD,²⁰ P4H,²⁵ CytC3,³² and by analogy DAOCS⁶⁸ and the histone demethylase KDM4E,⁶⁹ HAT by the ferryl or product release are partially rate-limiting on turnover at elevated O₂ concentration, preventing the accumulation of any species involved in O₂ activation during the pre-steady-state. A crucial difference between these other enzymes and FIH is that several lines of evidence indicate that decarboxylation is rate limiting in FIH, suggesting that FIH may allow direct access to steps involved in O₂ activation.

CONCLUSIONS

We have used multiple kinetic probes to characterize O₂ activation by FIH. Unlike other previously characterized Fe(II)/ α KG enzymes, turnover in FIH is fully limited by the rate of O₂ activation. This kinetic feature is consistent with the function of FIH as an O₂ sensor; strong oxidants such as the ferryl would be short-lived, ensuring tight coupling between O₂ activation and CTAD hydroxylation. It may be possible that other biomedically important Fe(II)/ α KG enzymes such as the JmjC and JmjD domain-containing hydroxylases and PHD2 employ a similar mechanistic strategy to regulate their function. If so, rate-limited O₂ activation may be a more common mechanistic feature among Fe(II)/ α KG oxygenases than is currently appreciated.

ASSOCIATED CONTENT

Supporting Information

Control experiments involving steady-state kinetics with the CTAD^{788–806} peptide, as well as steady-state kinetics in the presence and absence of ascorbate. The material is available free of charge via the Internet at <http://pubs.acs.org>.

AUTHOR INFORMATION

Corresponding Author

*E-mail: mknapp@chem.umass.edu. Voice: (413) 545-4001. Fax: (413) 545-4490.

Funding

This research was supported by the U.S. National Institutes of Health (Grant 1R01-GM077413 to M.J.K.) and the National Science Foundation (Grant EAR-1053432) to N.E.O. J.A.H. was supported in part by the NIH Chemistry-Biology Interface Predoctoral Training Grant T32-GM008515.

Notes

The authors declare no competing financial interest.

ABBREVIATIONS

ACCO, 1-aminocyclopropane-1-carboxylic acid oxidase; α KG, α -ketoglutarate; CAS, clavamate synthase; CTAD, C-terminal transactivation domain; DFT, density functional theory; EIE, equilibrium isotope effect; FIH, factor-inhibiting HIF; HAT, hydrogen atom transfer; HEPES, 4-(2-hydroxyethyl)-1-piperazineethanesulfonic acid; HIF, hypoxia inducible factor-1 α ; HppE, (S)-2-hydroxypropyl-1-phosphonate epoxidase; IRMS, isotope ratio mass spectrometry; KIE, kinetic isotope effect; MALDI-TOF-MS, matrix assisted laser desorption ionization-time-of-flight-mass spectrometry; MCD, magnetic circular dichroism; P4H, prolyl-4-hydroxylase; PHD2, prolyl hydrox-

ylase domain 2; SKIE, solvent kinetic isotope effect; SCF, self-consistent field; SOD, superoxide dismutase; TauD, taurine dioxygenase; TFA, trifluoroacetic acid; VTVH, variable temperature variable field

REFERENCES

- (1) Taabazuing, C. Y., Hangasky, J. A., and Knapp, M. J. (2014) Oxygen sensing strategies in mammals and bacteria. *J. Inorg. Biochem.* 133, 63–72.
- (2) Mole, D. R., Blancher, C., Copley, R. R., Pollard, P. J., Gleadle, J. M., Ragoussis, J., and Ratcliffe, P. J. (2009) Genome-wide Association of Hypoxia-inducible Factor (HIF)-1 α and HIF-2 α DNA Binding with Expression Profiling of Hypoxia-inducible Transcripts. *J. Biol. Chem.* 284, 16767–16775.
- (3) Ke, Q., and Costa, M. (2006) Hypoxia-Inducible Factor-1 (HIF-1). *Mol. Pharmacol.* 70, 1469–1480.
- (4) Semenza, G. L. (2003) Targeting HIF-1 for cancer therapy. *Nat. Rev. Cancer* 3, 721–732.
- (5) Metzzen, E., and Ratcliffe, P. J. (2004) HIF hydroxylation and cellular oxygen sensing. *Biol. Chem.* 385, 223–230.
- (6) Schofield, C. J., and Ratcliffe, P. J. (2004) Oxygen sensing by HIF-hydroxylases. *Nat. Rev. Mol. Cell Biol.* 5, 343–354.
- (7) Lando, D., Peet, D. J., Gorman, J. J., Whelan, D. A., Whitelaw, M. L., and Bruick, R. K. (2002) FIH-1 is an asparaginyl hydroxylase enzyme that regulates the transcriptional activity of hypoxia-inducible factor. *Genes Dev.* 16, 1466–1471.
- (8) McNeill, L. A., Hewitson, K. S., Claridge, T. D., Seibel, J. F., Horsfall, L. E., and Schofield, C. J. (2002) Hypoxia-inducible factor asparaginyl hydroxylase (FIH-1) catalyses hydroxylation at the beta-carbon of asparagine-803. *Biochem. J.* 367, 571–575.
- (9) Lando, D., Peet, D. J., Whelan, D. A., Gorman, J. J., and Whitelaw, M. L. (2002) Asparagine hydroxylation of the HIF transactivation domain a hypoxic switch. *Science* 295, 858–861.
- (10) Solomon, E. I., Light, K. M., Liu, L. V., Srncic, M., and Wong, S. D. (2013) Geometric and Electronic Structure Contributions to Function in Non-heme Iron Enzymes. *Acc. Chem. Res.* 46, 2725–2739.
- (11) Blomberg, M. R. A., Borowski, T., Himo, F., Liao, R. Z., and Siegbahn, P. E. M. (2014) Quantum Chemical Studies of Mechanisms for Metalloenzymes. *Chem. Rev.* 114, 3601–3658.
- (12) Hausinger, R. P. (2004) Fe(II)/ α -Ketoglutarate-dependent hydroxylases and related enzymes. *Crit. Rev. Biochem. Mol. Biol.* 39, 21–68.
- (13) Aik, W., McDonough, M. A., Thalhammer, A., Chowdhury, R., and Schofield, C. J. (2012) Role of the jelly-roll fold in substrate binding by 2-oxoglutarate oxygenases. *Curr. Opin. Struct. Biol.* 22, 691–700.
- (14) Bollinger, J. M., Price, J. C., Hoffart, L. M., Barr, E. W., and Krebs, C. (2005) Mechanism of Taurine: α -Ketoglutarate Dioxygenase (TauD) from *Escherichia coli*. *Eur. J. Inorg. Chem.* 2005, 4245–4254.
- (15) Grzyska, P. K., Appelman, E. H., Hausinger, R. P., and Proshlyakov, D. A. (2010) Insight into the mechanism of an iron dioxygenase by resolution of steps following the FeIV=HO species. *Proc. Natl. Acad. Sci. U. S. A.* 107, 3982–3987.
- (16) Light, K. M., Hangasky, J. A., Knapp, M. J., and Solomon, E. I. (2013) Spectroscopic Studies of the Mononuclear Non-Heme Fe-II Enzyme FIH: Second-Sphere Contributions to Reactivity. *J. Am. Chem. Soc.* 135, 9665–9674.
- (17) Neidig, M. L., Brown, C. D., Light, K. M., Fujimori, D. G., Nolan, E. M., Price, J. C., Barr, E. W., Bollinger, J. M., Krebs, C., Walsh, C. T., and Solomon, E. I. (2007) CD and MCD of CytC3 and taurine dioxygenase: role of the facial triad in α -KG-dependent oxygenases. *J. Am. Chem. Soc.* 129, 14224–14231.
- (18) Zhou, J., Kelly, W. L., Bachmann, B. O., Gunsior, M., Townsend, C. A., and Solomon, E. I. (2001) Spectroscopic studies of substrate interactions with clavamate synthase 2, a multifunctional α -KG-dependent non-heme iron enzyme: Correlation with mechanisms and reactivities. *J. Am. Chem. Soc.* 123, 7388–7398.

- (19) Price, J. C., Barr, E. W., Tirupati, B., Bollinger, J. M., and Krebs, C. (2003) The First Direct Characterization of a High-Valent Iron Intermediate in the Reaction of an α -Ketoglutarate-Dependent Dioxygenase: A High-Spin Fe(IV) Complex in Taurine/ α -Ketoglutarate Dioxygenase (TauD) from *Escherichia coli*. *Biochemistry* 42, 7497–7508.
- (20) Price, J. C., Barr, E. W., Glass, T. E., Krebs, C., and Bollinger, J. M. (2003) Evidence for Hydrogen Abstraction from C1 of Taurine by the High-Spin Fe(IV) Intermediate Detected during Oxygen Activation by Taurine: α -Ketoglutarate Dioxygenase (TauD). *J. Am. Chem. Soc.* 125, 13008–13009.
- (21) Riggs-Gelasco, P. J., Price, J. C., Guyer, R. B., Brehm, J. H., Barr, E. W., Bollinger, J. M., and Krebs, C. (2004) EXAFS spectroscopic evidence for an Fe = O unit in the Fe(IV) intermediate observed during oxygen activation by taurine: α -ketoglutarate dioxygenase. *J. Am. Chem. Soc.* 126, 8108–8109.
- (22) Grzyska, P. K., Ryle, M. J., Monterosso, G. R., Liu, J., Ballou, D. P., and Hausinger, R. P. (2005) Steady-State and Transient Kinetic Analyses of Taurine/ α -Ketoglutarate Dioxygenase: Effects of Oxygen Concentration, Alternative Sulfonates, and Active-Site Variants on the FeIV-oxo Intermediate. *Biochemistry* 44, 3845–3855.
- (23) Proshlyakov, D. A., Henshaw, T. F., Monterosso, G. R., Ryle, M. J., and Hausinger, R. P. (2004) Direct Detection of Oxygen Intermediates in the Non-Heme Fe Enzyme Taurine/ α -Ketoglutarate Dioxygenase. *J. Am. Chem. Soc.* 126, 1022–1023.
- (24) Ryle, M. J., Padmakumar, R., and Hausinger, R. P. (1999) Stopped-Flow Kinetic Analysis of *Escherichia coli* Taurine/ α -Ketoglutarate Dioxygenase: Interactions with α -Ketoglutarate, Taurine, and Oxygen. *Biochemistry* 38, 15278–15286.
- (25) Hoffart, L. M., Barr, E. W., Guyer, R. B., Bollinger, J. M., and Krebs, C. (2006) Direct spectroscopic detection of a C-H-cleaving high-spin Fe(IV) complex in a prolyl-4-hydroxylase. *Proc. Natl. Acad. Sci. U. S. A.* 103, 14738–14743.
- (26) Galonic Fujimori, D., Barr, E. W., Matthews, M. L., Koch, G. M., Yonce, J. R., Walsh, C. T., Bollinger, J. M., Jr., Krebs, C., and Riggs-Gelasco, P. J. (2007) Spectroscopic evidence for a high-spin Br-Fe(IV)-Oxo intermediate in the α -ketoglutarate-dependent halogenase CytC3 from *Streptomyces*. *J. Am. Chem. Soc.* 129, 13408–13409.
- (27) Wong, S. D., Srncic, M., Matthews, M. L., Liu, L. V., Kwak, Y., Park, K., Bell, C. B., III, Alp, E. E., Zhao, J., Yoda, Y., Kitao, S., Seto, M., Krebs, C., Bollinger, J. M., Jr., and Solomon, E. I. (2013) Elucidation of the Fe(IV)=O intermediate in the catalytic cycle of the halogenase SyrB2. *Nature* 499, 320–323.
- (28) Borowski, T., Bassan, A., and Siegbahn, P. E. M. (2004) Mechanism of dioxygen activation in 2-oxoglutarate-dependent enzymes: A hybrid DFT study. *Chem.—Eur. J.* 10, 1031–1041.
- (29) Ye, S., Riplinger, C., Hansen, A., Krebs, C., Bollinger, J. M., and Neese, F. (2012) Electronic Structure Analysis of the Oxygen-Activation Mechanism by FeII- and α -Ketoglutarate (α KG)-Dependent Dioxygenases. *Chem.—Eur. J.* 18, 6555–6567.
- (30) Topol, I. A., Nemukhin, A. V., Salnikow, K., Cachau, R. E., Abashkin, Y. G., Kasprzak, K. S., and Burt, S. K. (2006) Quantum chemical modeling of reaction mechanism for 2-oxoglutarate dependent enzymes: effect of substitution of iron by nickel and cobalt. *J. Phys. Chem. A* 110, 4223–4428.
- (31) Mirica, L. M., McCusker, K. P., Munos, J. W., Liu, H., and Klinman, J. P. (2008) ^{18}O kinetic isotope effects in non-heme iron enzymes: Probing the nature of Fe/O₂ intermediates. *J. Am. Chem. Soc.* 130, 8122–8123.
- (32) Galonic, D. P., Barr, E. W., Walsh, C. T., Bollinger, J. M., Jr., and Krebs, C. (2007) Two interconverting Fe(IV) intermediates in aliphatic chlorination by the halogenase CytC3. *Nat. Chem. Biol.* 3, 113–116.
- (33) Price, J. C., Barr, E. W., Hoffart, L. M., Krebs, C., and Bollinger, J. M. (2005) Kinetic dissection of the catalytic mechanism of taurine: α -ketoglutarate dioxygenase (TauD) from *Escherichia coli*. *Biochemistry* 44, 8138–8147.
- (34) Hangasky, J. A., Saban, E., and Knapp, M. J. (2013) Inverse Solvent Isotope Effects Arising from Substrate Triggering in the Factor Inhibiting Hypoxia Inducible Factor. *Biochemistry* 52, 1594–1602.
- (35) Chen, Y. H., Comeaux, L. M., Herbst, R. W., Saban, E., Kennedy, D. C., Maroney, M. J., and Knapp, M. J. (2008) Coordination changes and auto-hydroxylation of FIH-1: Uncoupled O-2-activation in a human hypoxia sensor. *J. Inorg. Biochem.* 102, 2120–2129.
- (36) (1981) *CRC Handbook of Chemistry and Physics*, 61st ed., CRC Press, Boca Raton, FL.
- (37) Emerson, S., Quay, P., Stump, C., Wilbur, D., and Knox, M. (1991) Oxygen Argon Nitrogen and Radon-222 in Surface Waters of the Subarctic Ocean Net Biological Oxygen Production. *Global Biogeochem. Cycles* 5, 49–70.
- (38) Roberts, B. J., Russ, M. E., and Ostrom, N. E. (2000) Rapid and Precise Determination of the $\delta^{18}\text{O}$ of Dissolved and Gaseous Dioxygen via Gas Chromatography–Isotope Ratio Mass Spectrometry. *Environ. Sci. Technol.* 34, 2337–2341.
- (39) Dansgaard, W. (1964) Stable Isotopes in Precipitation. *Tellus* 16, 436–468.
- (40) Barkan, E., and Luz, B. (2005) High precision measurements of O-17/O-16 and O-18/O-16 ratios in H₂O. *Rapid Commun. Mass Spectrom.* 19, 3737–3742.
- (41) Nagel, S., Talbot, N. P., Mecinovic, J., Smith, T. G., Buchan, A. M., and Schofield, C. J. (2010) Therapeutic manipulation of the HIF hydroxylases. *Antioxid. Redox Signal.* 12, 481–501.
- (42) Semenza, G. L. (2009) Regulation of Oxygen Homeostasis by Hypoxia-Inducible Factor 1. *Physiology* 24, 97–106.
- (43) Simmons, J. M., Muller, T. A., and Hausinger, R. P. (2008) FeII/ α -ketoglutarate hydroxylases involved in nucleobase, nucleoside, nucleotide, and chromatin metabolism. *Dalton Trans.*, 5132–5142.
- (44) Zheng, G., Fu, Y., and He, C. (2014) Nucleic Acid Oxidation in DNA Damage Repair and Epigenetics. *Chem. Rev.* 114, 4602–4620.
- (45) Ehrismann, D., Flashman, E., Genn, D. N., Mathioudakis, N., Hewitson, K. S., Ratcliffe, P. J., and Schofield, C. J. (2007) Studies on the activity of the hypoxia-inducible-factor hydroxylases using an oxygen consumption assay. *Biochem. J.* 401, 227–234.
- (46) Koivunen, P., Hirsilä, M., Günzler, V., Kivirikko, K. I., and Myllyharju, J. (2004) Catalytic properties of the asparaginyl hydroxylase (FIH) in the oxygen sensing pathway are distinct from those of its prolyl 4-hydroxylases. *J. Biol. Chem.* 279, 9899–9904.
- (47) Ryle, M. J., Padmakumar, R., and Hausinger, R. P. (1999) Stopped-flow kinetic analysis of *Escherichia coli* taurine/ α -ketoglutarate dioxygenase: Interactions with α -ketoglutarate, taurine, and oxygen. *Biochemistry* 38, 15278–15286.
- (48) Fitzpatrick, P. F. (1991) Steady-state kinetic mechanism of rat tyrosine-hydroxylase. *Biochemistry* 30, 3658–3662.
- (49) Saam, J., Ivanov, I., Walther, M., Holzhütter, H. G., and Kuhn, H. (2007) Molecular dioxygen enters the active site of 12/15-lipoxygenase via dynamic oxygen access channels. *Proc. Natl. Acad. Sci. U. S. A.* 104, 13319–13324.
- (50) Knapp, M. J., and Klinman, J. P. (2003) Kinetic studies of oxygen reactivity in soybean lipoxygenase-1. *Biochemistry* 42, 11466–11475.
- (51) Hirsilä, M., Koivunen, P., Günzler, V., Kivirikko, K. I., and Myllyharju, J. (2003) Characterization of the human prolyl 4-hydroxylases that modify the hypoxia-inducible factor. *J. Biol. Chem.* 278, 30772–30780.
- (52) Cascella, B., and Mirica, L. M. (2012) Kinetic Analysis of Iron-Dependent Histone Demethylases: α -Ketoglutarate Substrate Inhibition and Potential Relevance to the Regulation of Histone Demethylation in Cancer Cells. *Biochemistry* 51, 8699–8701.
- (53) Fielden, E. M., Roberts, P. B., Bray, R. C., Lowe, D. J., Mautner, G. N., Rotilio, G., and Calabres, L. (1974) Mechanism of action of Superoxide-Dismutase from pulse-radiolysis and electron-paramagnetic resonance-evidence that only half active-sites function in catalysis. *Biochem. J.* 139, 49–60.

(54) Rotilio, G., Bray, R. C., and Fielden, E. M. (1972) A pulse radiolysis study of superoxide dismutase. *Biochim. Biophys. Acta, Enzymol.* 268, 605–609.

(55) Hasinoff, B. B. (1984) Kinetics of Carbonic-Anhydrase in Solvents of Increased Viscosity - A Partially Diffusion-Controlled Reaction. *Arch. Biochem. Biophys.* 233, 676–681.

(56) Pocker, Y., and Janjic, N. (1987) Enzyme-Kinetics in Solvents of Increased Viscosity - Dynamic Aspects of Carbonic-Anhydrase Catalysis. *Biochemistry* 26, 2597–2606.

(57) Perry, J. J. P., Shin, D. S., Getzoff, E. D., and Tainer, J. A. (2010) The structural biochemistry of the superoxide dismutases. *Biochim. Biophys. Acta, Proteins Proteomics* 1804, 245–262.

(58) Tian, G., and Klinman, J. P. (1993) Discrimination between ^{16}O and ^{18}O in Oxygen Binding to the Reversible Oxygen Carriers Hemoglobin, Hemerythrin, and Hemocyanin: A new Probe for Oxygen Binding and Reductive Activation by Proteins. *J. Am. Chem. Soc.* 115, 8891–8897.

(59) Tian, G., Berry, J., and Klinman, J. (1994) Oxygen-18 Kinetic Isotope Effects in the Dopamine β -Monooxygenase Reaction: Evidence for a New Chemical Mechanism in Non-Heme Metallomonooxygenases. *Biochemistry* 33, 226–234.

(60) Roth, J. P. (2007) Advances in studying bioinorganic reaction mechanisms: Isotopic probes of activated oxygen intermediates in metalloenzymes. *Curr. Opin. Chem. Biol.* 11, 142–150.

(61) Stahl, S. S., Francisco, W. a, Merckx, M., Klinman, J. P., and Lippard, S. J. (2001) Oxygen kinetic isotope effects in soluble methane monooxygenase. *J. Biol. Chem.* 276, 4549–4553.

(62) Mirica, L. M., and Klinman, J. P. (2008) The nature of O_2 activation by the ethylene-forming enzyme 1-aminocyclopropane-1-carboxylic acid oxidase. *Proc. Natl. Acad. Sci. U. S. A.* 105, 1814–1819.

(63) Francisco, W. A., Tian, G. C., Fitzpatrick, P. F., and Klinman, J. P. (1998) Oxygen-18 kinetic isotope effect studies of the tyrosine hydroxylase reaction: Evidence of rate limiting oxygen activation. *J. Am. Chem. Soc.* 120, 4057–4062.

(64) Hotopp, J. C. D., and Hausinger, R. P. (2002) Probing the 2,4-dichlorophenoxyacetate/ α -ketoglutarate dioxygenase substrate-binding site by site-directed mutagenesis and mechanism-based inactivation. *Biochemistry* 41, 9787–9794.

(65) Thornburg, L. D., Lai, M. T., Wishnok, J. S., and Stubbe, J. (1993) A non-heme iron protein with heme tendencies: An investigation of the substrate specificity of thymine hydroxylase. *Biochemistry* 32, 14023–14033.

(66) Saban, E., Chen, Y. H., Hangasky, J., Taabazuing, C., Holmes, B., and Knapp, M. (2011) The second coordination sphere of FIH controls hydroxylation. *Biochemistry* 50, 4733–4740.

(67) Flagg, S. C., Giri, N., Pektas, S., Maroney, M. J., and Knapp, M. J. (2012) Inverse Solvent Isotope Effects Demonstrate Slow Aquo Release from Hypoxia Inducible Factor-Prolyl Hydroxylase (PHD2). *Biochemistry* 51, 6654–6666.

(68) Tarhonskaya, H., Szöllössi, A., Leung, I. K. H., Bush, J. T., Henry, L., Chowdhury, R., Iqbal, A., Claridge, T. D. W., Schofield, C. J., and Flashman, E. (2014) Studies on Deacetoxycephalosporin C Synthase Support a Consensus Mechanism for 2-Oxoglutarate Dependent Oxygenases. *Biochemistry* 53, 2483–2493.

(69) Sanchez-Fernandez, E. M., Tarhonskaya, H., Al-Qahtani, K., Hopkinson, R. J., McCullagh, J. S., Schofield, C. J., and Flashman, E. (2013) Investigations on the oxygen dependence of a 2-oxoglutarate histone demethylase. *Biochem. J.* 449, 491–496.